Getting more out of an incommensurately modulated structure: the example of $K_5Yb(MoO_4)_4$

Alla Arakcheeva and Gervais Chapuis

research papers

Getting more out of an incommensurately modulated structure: the example of $K_5Yb(MoO_4)_4$

Alla Arakcheeva and Gervais Chapuis*

École Polytechnique Fédérale de Lausanne,
Laboratoire de cristallographie, BSP, CH-1015
Lausanne, Switzerland

Correspondence e-mail:
gervais.chapuis@epfl.ch

A method based on the superspace approach is presented with the aim of generating a family of modular structures from a single incommensurately modulated structure. This approach based on the variation of the modulation vector $\mathbf{q}$ is applied to the generation of the $K_5Yb(MoO_4)_4$, potassium ytterbium tetramolybdate, family of modular structures. The β coefficient of the modulation vector $\mathbf{q} = \beta\mathbf{b}^*$ is a temperature-dependent variable which determines the modification. Our method gives a unified frame to describe and explain the three temperature-dependent phases of $K_5Yb(MoO_4)_4$. Phase β can be represented as a polytypic modification with $1/2\mathbf{b}^* \leq \mathbf{q} \leq 2/3\mathbf{b}^*$; phases γ ($\mathbf{q} = 1/2\mathbf{b}^*$) and α ($\mathbf{q} = 1\mathbf{b}^*$) are the lowest and the highest temperature members of the $K_5Yb(MoO_4)_4$ family, respectively.

1. Introduction

The concept of superspace, *i.e.* the theoretical framework describing the symmetry of non-periodic crystalline structures in a space of dimensions larger than three, has been very successful in describing incommensurate and composite structures (see for example the special issue dedicated to aperiodic structures in *Z. Kristallogr.* **219**, 2004). The key to its success lies in the ability to recover lattice periodicity by describing the structures in higher than three-dimensional space. It is now universally applied for the description of various types of aperiodic structures. Recently, however, the domain of applications of the superspace concept has been further extended and new possibilities of applications are still being explored. One of the most recent developments is associated with the description of families of modular structures. In this approach a family of modular structures can be described in terms of various three-dimensional sections of a virtual $(3 + 1)$-dimensional modulated structure (see, for example, Lind & Lidin, 2003; Elcoro *et al.*, 2003). The method consists of first extracting the basic modules and their arrangements from all known members of a structural family. In the second step a common parent model is derived in superspace such that all the members of the family can be deduced by setting the modulation vector $\mathbf{q}$ to specific rational or irrational values.

In the present work, we propose a new approach based on the superspace formalism in order to generate a family of modular structures. Starting from a single known incommensurately modulated structure of the family we shall describe a method to generate all the possible phases which might occur by exploring the possibilities offered by the superspace symmetry description. By varying the modulation vector of

electronic reprint

the known incommensurate structure we are able to generate a complete family of modular structures. We show that not only the symmetry and the topological description can be determined, but also the complete set of atomic parameters can be deduced for every member of the family. Moreover, further information on the most probable members of the family can be extracted from the incommensurate structure. In addition, it is shown how this information helps to explain the experimental data on the temperature-dependent non-equilibrium phase transformation. The space groups of the commensurate members of the generated family can be selected among the three-dimensional subgroups of the superspace group of the parent aperiodic structure. For this purpose, we apply the *Superspace Group Finder* (Orlov *et al.*, 2004) or the *JANA*2000 program (Petricek & Dusek, 2000).

The proposed method is illustrated with the example of the incommensurately modulated structure β-K$_5$Yb(MoO$_4$)$_4$, which will be considered as the parent structure. Three known modifications of this complex molybdenum oxide belonging to the palmierite [K$_2$Pb(SO$_4$)$_2$] structure type were recently described (Morozov *et al.*, 2003; Arakcheeva *et al.*, 2005):

(i) the high-temperature phase α, space group $R\bar{3}m$, $a = 6.0372$ (1), $c = 20.4045$ (2) Å;

(ii) the low-temperature phase γ, space group $C2/c$, $a = 14.8236$ (1), $b = 12.1293$ (1), $c = 10.5151$ (1) Å, $\beta = 114.559$ (1)°;

(iii) the intermediate incommensurately modulated phase β, superspace group $X2/m(0\beta0)00$, where $X = [\frac{1}{2}\frac{1}{2} 0\, 0;\, 0\, 0\, \frac{1}{2}\frac{1}{2};\, \frac{1}{2}\frac{1}{2}$ $\frac{1}{2}\frac{1}{2}]$, $a = 10.4054$ (16), $b = 6.1157$ (12), $c = 19.7751$ (18), $\beta = 136.625$ (10)°, **q** = 0.6354 (3)**b***.

The crystal structures of phases α and γ were refined by Morozov *et al.* (2003). The refinement of the β-phase structure (Arakcheeva *et al.*, 2005) provides a basis for the present publication.

2. Experimental data on K$_5$Yb(MoO$_4$)$_4$

In order to illustrate the new method of analysis and interpretation, we briefly summarize the experimental evidence available on K$_5$Yb(MoO$_4$)$_4$ from publications.

2.1. Characteristic features of the preparation and phase transformations

The temperature-dependent phase transition $\alpha \Rightarrow \beta \leftrightarrow \gamma$ was reported by Morozov *et al.* (2003). The low-temperature modification γ prepared at 893 ± 10 K is also stable at lower temperature. Annealing of this modification at 960 ± 10 K (close to the melting point) followed by a quick quenching to liquid nitrogen freezes the high-temperature α modification. Slow cooling from 960 K to room temperature (RT) results in the formation of modification β and points to the $\alpha \Rightarrow \beta$ transformation. No $\beta \Rightarrow \gamma$ transformation was observed during this experiment. Differential scanning calorimetry (DDSC) studies carried out in the 293–1013 K temperature range (Morozov *et al.*, 2003) shows that the phase transitions are associated with minor reconstructions of the crystal structures. Calculated DSC curves show a weak effect associated with only the $\alpha \leftrightarrow \beta$ transformation (Fig. 2 in Morozov *et al.*, 2003).

2.2. Crystal structure description

All three K$_5$Yb(MoO$_4$)$_4$ modifications belong to the palmierite structure type. In order to extract the essential features of these phases, it is best to represent the structures as built from [MMo$_6$K$_2$] cubic clusters (M clusters) centred by the M atom, where M is K, Yb or a mixture (K$_{0.5}$Yb$_{0.5}$); Mo lies at the centre of the MoO$_4$ tetrahedron (Fig. 1).
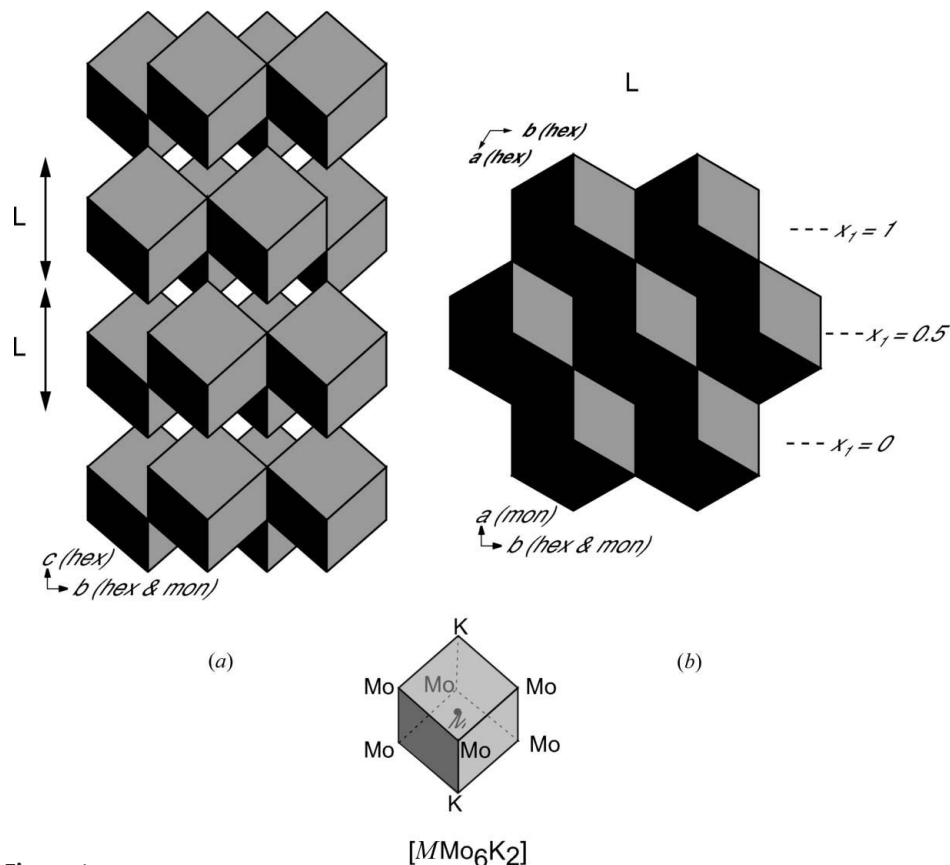

Figure 1
The palmierite structure type represented in terms of [MMo$_6$K$_2$] cubic clusters (M can be K, Yb or a mixed position). O atoms forming MoO$_4$ tetrahedra are missing. (*a*) Projection of the structure in the $(yz)_{hex}$ plane with an indication of the layers *L*. (*b*) Representation of a single layer *L*. The monoclinic axes and values of $x = x_1$ correspond to the coordinate system of the incommensurate β phase. Details of a single cluster are also illustrated.

Table 1
Atomic parameters of the simulated phase Δ compared with the experimental data.

Atom	x Sim.	x Exp.	y Sim.	y Exp.	z Sim.	z Exp.	B_{iso} Sim.	B_{iso} Exp.
Yb	0	0.1256	0.1190 (2)	0.25		1.19	0.98	
K1	0.5	0.1194	0.1132 (2)	0.25		1.16	3.9	
K2	0.2899	0.2941 (3)	0.3651	0.3714 (6)	0.9433	0.9320 (4)	2.52	2.7
K3	0.2855	0.2841 (3)	0.8878	0.8944 (5)	0.9392	0.9401 (5)	2.52	2.8
Mo1	0.1014	0.1035 (1)	0.3724	0.3680 (2)	0.1627	0.1550 (2)	1.13	1.15
Mo2	0.0887	0.0913 (1)	0.8723	0.8667 (2)	0.1400	0.1390(2)	1.13	0.97
O11	0.9812	0.9863 (9)	0.4056	0.4027 (11)	0.0792	0.0753 (12)	2.39	3.7
O12	0.1635	0.1654 (9)	0.4821	0.4690 (9)	0.2728	0.2752 (12)	2.18	2.3
O13	0.1443	0.1495 (6)	0.3538	0.3797 (12)	0.0333	0.0305 (9)	2.43	1.9
O14	0.1114	0.1126 (9)	0.2494	0.2328 (8)	0.2588	0.2327 (11)	2.18	1.3
O21	0.9688	0.9741 (8)	0.8314	0.8216 (8)	0.0926	0.0992 (11)	2.39	0.7
O22	0.1037	0.1056 (6)	0.8895	0.8914 (11)	0.9828	0.9894 (9)	2.43	2.1
O23	0.1063	0.0959 (9)	0.9996	0.9839 (9)	0.2251	0.2324 (12)	2.18	3.5
O24	0.1705	0.1662 (8)	0.7669	0.7649 (9)	0.2539	0.2342 (13)	2.18	1.6

In all three modifications, the clusters form layers (Fig. 1b) stacked normal to the $\mathbf{c}_\alpha$ axis (Fig. 1a). If we neglect the cluster occupation, all layers L are equivalent by translation according to the symmetry of the rhombohedral α phase.

In the α phase all clusters have the composition $M = (K_{0.5}Yb_{0.5})$, whereas in the monoclinic β and γ phases, we observe an ordering of K and Yb in the center of the M clusters. According to our investigation of phase β, $\sim$ 2.5% of the M clusters exhibit a mixed $(K_{0.5},Yb_{0.5})$ composition.

The distribution of Yb and K in the structure is specific for each member of the $K_5Yb(MoO_4)_4$ modular family and thus each layer L can be used as a characteristic representative of each member of the family of structures. In the next section, we shall describe the representative layers L of phases α, β and γ and illustrate the method which generates the other structures of the same family.

3. Superspace approach applied to the generation of the $K_5Yb(MoO_4)_4$ modular structure family and analysis of the phase transformations

3.1. Generation of modular structure family

3.1.1. Method. The incommensurate structure of the monoclinic β phase (Table 1) is used as a generating structure for the deduction of the $K_5Yb(MoO_4)_4$ family. We first observe that all layer types L can be described by different arrangements of K, Yb or a mixture, $(K_{0.5}Yb_{0.5})$ in the centres of the M clusters located along $\mathbf{b}$ with $x_1 = 0$ and $\frac{1}{2}$ (Fig. 1b). From the x_2x_4 ($x_1 = 0$ and $\frac{1}{2}$, $x_3 = 0$) section of the refined structure β (Fig. 2a), the different arrangements can be generated from various sections parallel to $\mathbf{b}$ and normal to x_4 with different modulation vectors $\mathbf{q}$. For instance, the layers L characteristic of phases γ and α are represented in Figs. 2(b) and (c), respectively. In general, a rational (irrational) value of $\mathbf{q}$ refers to a commensurate (incommensurate) structure. For incommensurate structures, a specific aperiodic arrangement of the cations in the centres of the M clusters is uniquely determined by the corresponding value of $\mathbf{q}$. For commensurate structures,

any periodic arrangement and its corresponding space group not only depend on the value of the modulation vector $\mathbf{q}$, but also on the value of t_0 along x_4. We also observe that parameter b of the unit cell is defined by the magnitude of the modulation vector $\mathbf{q}$ (Fig. 2).

In the general commensurate case: $\mathbf{q} = n/k\mathbf{b}^*$, where n and k are integers; the monoclinic unit-cell parameters are $a \simeq a_\beta$, $c \simeq c_\beta$, $b \simeq kb_\beta$, $\beta \simeq \beta_\beta$ (the precise values of the unit-cell parameters cannot be simulated); the space group is $X121$, with lattice type $X = I$, A, C or P, depending on the value of $\mathbf{q}$ (Orlov *et al.*, 2004). If $t_0 = 0$, the symmetry operations related to the monoclinic $\mathbf{b}$ axis are $2/m$; if $t_0 = 1/4k$, the corresponding elements of symmetry can be $2/c$ or $2/a$. Using the *JANA*2000 system of programs (Petricek & Dusek, 2000), the atomic coordinates for all atoms can be deduced from three-dimensional sections with specific $\mathbf{q}$ and t_0 values from the generating model of the incommensurate structure β. Thus, a new commensurate structure is derived by keeping the refined structural parameters of phase β, and varying only the modulated vector $\mathbf{q}$ and value of t_0. All the atomic parameters follow from the corresponding t sections of structure β.

3.1.2. Confirmation of the validity of the method. The efficiency of this technique was tested for the structures of phase γ and α in relation to the experimental data. Some other commensurate models generated by the same method and represented by means of the corresponding layer L are also illustrated in Fig. 3 along with the parent incommensurate structure β (Fig. 3c).

The case where $\mathbf{q} = 1/2\mathbf{b}^*$ and $t_0 = 1/8$ (Figs. 2b and 3e, left) reproduces the structure of phase γ (space group $A2/a$; $b \simeq 2b_\beta$). The atomic parameters generated by the method were transformed in order to correspond to the published unit cell (Table 1). The generated values of the atomic coordinates are close to those of the published structure refined by the Rietveld method. The contributions of the atomic parameters to the powder diffraction patterns calculated for the simulated (Fig. 4a) and published (Fig. 4b) structures are nearly identical.

The case where $\mathbf{q} = 1\mathbf{b}^*$ and $t_0 = 1/4$ (Fig. 2c and 3a) corresponds to a commensurate monoclinic structure (space group $I2/c$, $b \simeq b_\beta$) with disordered cation positions $M = (K_{0.5}Yb_{0.5})$. This simulated model was considered for the description of phase α using our approach. For the calculation of the powder diffraction pattern, the monoclinic unit-cell parameters obtained from the transformed hexagonal unit-cell parameters of the rhombohedral phase α were used. A comparison of the calculated powder diffraction patterns derived from the simulation (Fig. 5a) and the published atomic parameters (Fig. 5b) shows identical patterns. In the hexagonal unit cell, the simulated model consists of split-atom positions (Table 2). In the refined rhombohedral α structure, the splitting (Δd) of the atom is compensated by a corresponding displacement parameter B_{iso}. The smallest Δd value

obtained from the simulated model, 0.17 Å for M and 0.15 Å for Mo, fits the experimental measurements $B_{iso} = 1$ Å^2; for K2, $\Delta d = 0.39$ Å, which is also close to the experimental measurement $B_{iso} = 3.6$ Å^2. The largest $\Delta d = 1.04$ Å for O1 and 1.92 Å for O2 explains the unusually high displacement parameter $B_{iso} = 8.9$ Å^2. Thus, the simulated monoclinic model is a good approximation of the rhombohedral structure α, *i.e.* the monoclinic atomic displacements forming domains connected by the threefold axis are able to explain the high values of the displacive parameters published for the rhombohedral α phase.

In order to confirm the validity of our method we performed the refinement of the **q** vector on the powder data kindly provided to us by V. Morozov using the atomic parameters obtained experimentally for the single crystal. In spite of similar thermal treatment used for the single crystal and powder sample preparation, the value $q = 0.6345\,(1)$ (powder) differs slightly from $q = 0.6354\,(30)$ (single crystal). The value $R_{all} = 0.079$ for all reflections (main and satellites of first, second and third orders) for the powder diffraction pattern is close to the corresponding value $R_{all} = 0.077$ obtained for the single-crystal experiment.

Therefore, the atomic parameters referring to different **q** vectors can be derived from only one incommensurate structure.

3.2. The derivation of the most probable modifications

In phase β the distribution of K, Yb and $(K_{0.5}Yb_{0.5})$ in the M clusters of layer L is aperiodic along **b** (Figs. 2a and 3c). However, the ordering of the distribution results from very subtle interactions between the edge-sharing M clusters represented in Fig. 1. Each MoO_4 tetrahedron is close to three M atoms at the centres of the clusters. Consequently, four O atoms participate in the coordination sphere of three M atoms. This asymmetry generates different orientations of the tetrahedra depending on the nature of the cation located at the centre of the M cluster (Fig. 6). In phase β the vicinity of every M cluster determines the orientation of every MoO_4 tetrahedron and consequently the optimal coordination number (CN) of the first coordination sphere of the M atom. For $M =$ Yb and $(K_{0.5}Yb_{0.5})$, the CN is always equal to 6; while for $M =$ K, the CN can be 8, 10 or 12 depending on the M cluster occupations in the vicinity (Figs. 3c and 6).

We postulate that the most probable structures can be selected among all the possible generated modifications on the basis that a portion of this structure exists in structure β. The corresponding configurations of the M cluster environment (illustrated in Fig. 3c) are determined by the occupation of the M position along the b axis (Fig. 2a). In order to select the most probable structure, the following formal rules characteristic of a local sequence of the M-position occupations in layer L of phase β can be formulated.

(i) The number of successive K or Yb atoms appearing along **b** cannot exceed 2 [first rule of the occupation sequence (hereafter OS-1)]. This rule is clear from Fig. 2(a): the difference Δx_4 between two neighbouring M positions is equal

to $0.5q = 0.3177$. This is shorter than $\Delta x_4 = 0.5$, which characterizes the switch of the M position occupancy along **b**. Therefore, two successive M positions can be occupied by the same type of atom. The third M position should switch the occupancy, because Δx_4 between the first and the third position is equal to $\mathbf{q} = 0.6354 > 0.5$.

(ii) The number of successive M positions occupied alternatively by K and Yb cannot exceed 3 [second rule of the occupation sequence (OS-2)]. The proof is similar to the first rule.

(iii) The mixed occupation $M = (Yb_{0.5}K_{0.5})$ can appear in a sequence as a substitute for one of the two uniformly occupied M positions [rule of replacement (RP)].
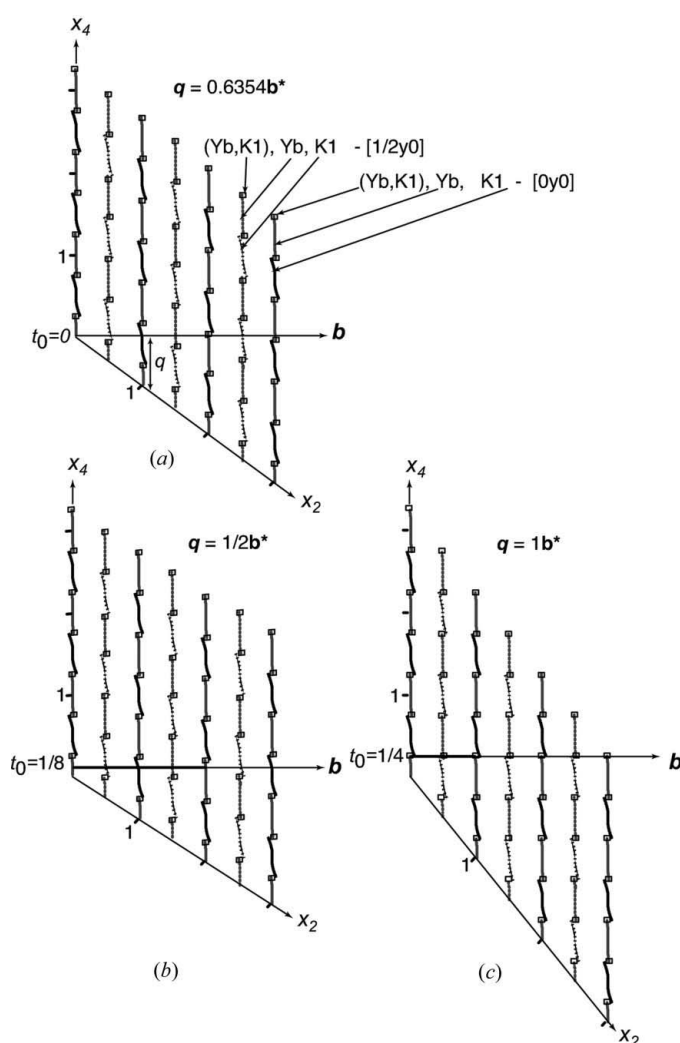

Figure 2
Occupation modulation of the M position in the x_2x_4 section ($x_3 = 0$; $x_1 = 0$ and 1/2) of (a) the incommensurate β-$K_5Yb(MoO_4)_4$ structure and its reconstructions for $\mathbf{q} = \frac{1}{2}\mathbf{b}^*$ (b) and $\mathbf{q} = 1\mathbf{b}^*$ (c). Solid and dashed lines refer to position with $x_1 = 0$ and $\frac{1}{2}$, respectively. Along the b axis, the sequence of K and Yb atoms defines their arrangement in layer L: (a) the aperiodic sequence [...$Yb_0K_{0.5}Yb_0(Yb,K)_{0.5}K_0Yb_{0.5}Yb_0$...] is characteristic of the M position of phase β; (b) the periodic sequence [$K_0K_{0.5}Yb_0Yb_{0.5}$] reproduces the data published for phase γ ($b_\gamma = 2b_\beta$); (c) the periodic sequence of $M = (K_{0.5}Yb_{0.5})$ is closely related to the data published for phase α ($b_\alpha = b_\beta$).

(iv) The composition of a single L layer should be equal to the composition of the compound [rule of randomly distributed density (RDD)]. This is a consequence of the fact that all L layers are symmetrically equivalent in structure β.

A selection of the most probable structures is illustrated in Fig. 7. The main characteristics of the selected structures are shown in Fig. 3.

According to rule OS-1, one limiting structure is described as the $[K_0K_{0.5}Yb_0Yb_{0.5}]$ sequence of the M cluster along $\mathbf{b}$, where the index refers to the x coordinate. This corresponds to structure γ ($\mathbf{q} = \frac{1}{2}\mathbf{b}^*$, $t_0 = 1/8$; Fig. 3e, left]. Alternatively, according to rule RP, the structure $[K_0(K,Yb)_{0.5}Yb_0(K,Yb)_{0.5}]$ ($\mathbf{q} = 1/2\mathbf{b}^*$, $t_0 = 0$; Fig. 3e, right) can also be a limiting case. Thus, $\mathbf{q} = 1/2\mathbf{b}^*$ is the lower limit o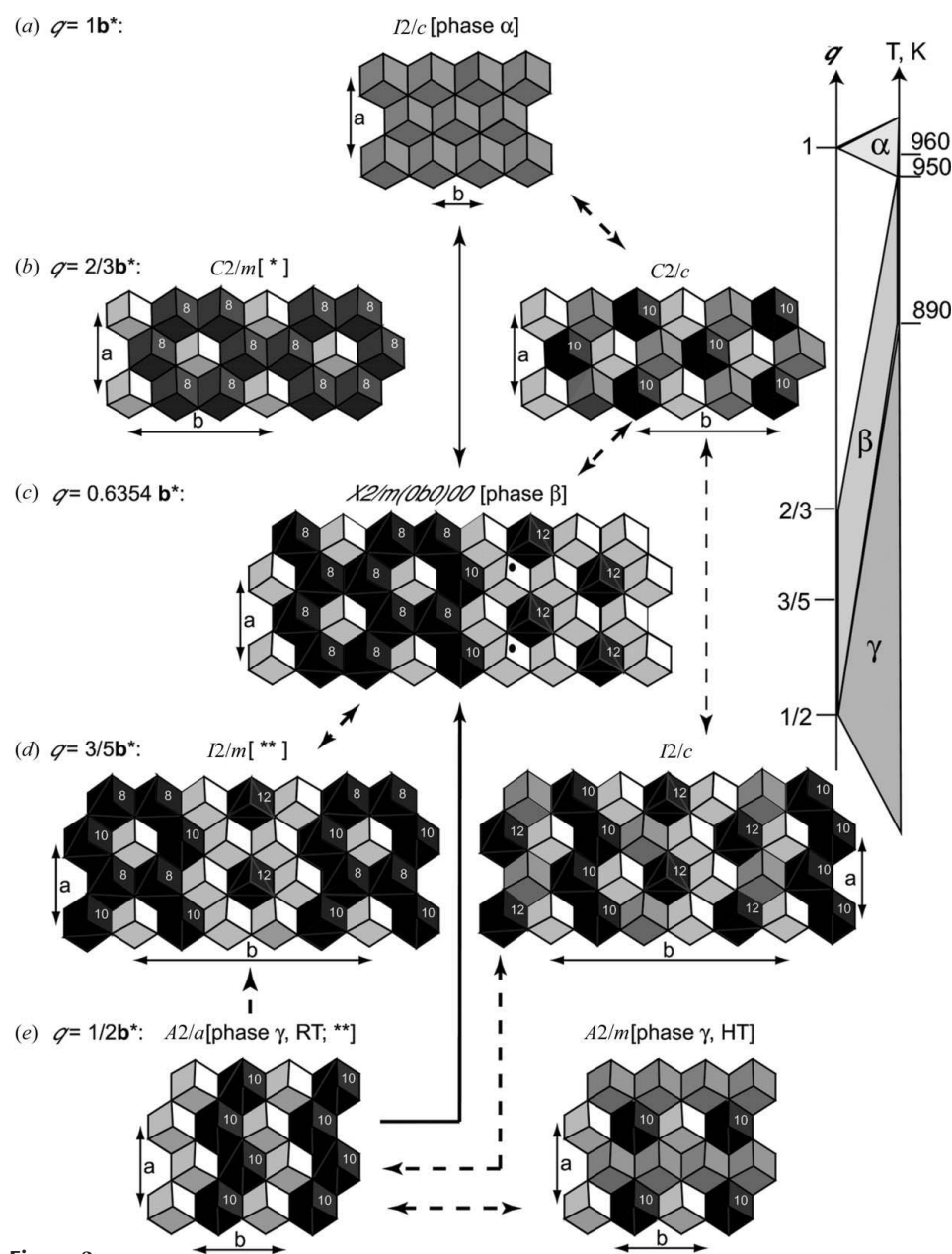f the most probable modification. According to rule OS-2, the other limiting structure corresponds to the sequence $[K_0Yb_{0.5}Yb_0K_{0.5}Yb_0Yb_{0.5}]$ ($\mathbf{q} = 2/3\mathbf{b}^*$, $t_0 = 0$; Fig. 3b, left). Again, according to rule RP, the structure $[K_0Yb_{0.5}(K,Yb)_0K_{0.5}Yb_0(K,Yb)_{0.5}]$ ($\mathbf{q} = 2/3\mathbf{b}^*$, $t_0 = 1/4$; Fig. 3b, right) is also a possible limiting case. Therefore, $\mathbf{q} = 2/3\mathbf{b}^*$ is the upper limit of the most probable modification. However, according to rule RDD, the $[K_0Yb_{0.5}Yb_0K_{0.5}Yb_0Yb_{0.5}]$ structure can be excluded from the most probable structures, because in this case, two adjacent L layers have different compositions, K/Yb = $\frac{1}{2}$ and Yb/K = $\frac{1}{2}$, as they are symmetrically independent. Hence, the only $[K_0Yb_{0.5}(K,Yb)_0K_{0.5}Yb_0(K,Yb)_{0.5}]$ commensurate structure refers to the limiting case where $\mathbf{q} = 2/3\mathbf{b}^*$. All other commensurate and incommensurate structures defined in the range $1/2\mathbf{b}^* < \mathbf{q} < 2/3\mathbf{b}^*$ are the most probable modifications. All these modifications can be considered as belonging to the same polytypic family.

Structure α, $[(K,Yb)_0(K,Yb)_{0.5}]$ ($\mathbf{q} = 1\mathbf{b}^*$, $t_0 = 1/4$; Fig. 3a and 2c), can be included in this group as a degenerate case containing only disordered M positions.

4. Experimental and predicted phase transformations

Using our previous analysis and the experimental data described in §2.1, we suggest the general scheme of phase transformation, which can be described in correlation with the temperature variation of the modulation vector $\mathbf{q}$ (Fig. 3). We also assume that by decreasing the temperature the ordering of the K and Yb atoms increases in the M clusters.

Figure 3
Structure characteristics of L layers for some simulated commensurate polytypes (a, b, d, e) along with the parent incommensurate structure β (c). The structures are represented according to their $\mathbf{q}$ value and their corresponding temperature of stabilization, both indicated at the upper right part of the figure. The solid and dashed arrows indicate the experimentally observed and the proposed temperature-dependent phase transformations, respectively. The experimentally observed structures are defined as α, β and γ, all others are predicted. In the L layers: K, Yb and (K,Yb) clusters are shown in black, white and grey. The white numbers indicate the CN of the K atom in the first coordination sphere. The black circles in structure β indicate the locations of the Yb clusters allowing mixed (K,Yb) composition. * and ** refer to the least probable and the lock-in modifications, respectively.

Table 2
Atomic parameters of the simulated phase Δ compared with the published data (space group $R\bar{3}m$).

Atom	x		y		z		B_{iso}	
	Sim.	Exp.	Sim.	Exp.	Sim.	Exp.	Sim.	Exp.
M	0	−0.01435	0	0	1.17	0.98		
K2	−0.0065	0	−0.0356	0	0.1878	0.1954 (2)	2.52	3.6
Mo	−0.0144	0	−0.0109	0	0.3961	0.3989 (1)	1.13	1.09
O1	−0.0686	0	0.0427	0	0.3162	0.3181 (5)	2.18	8.9
O2	(i) −0.1152	−0.1694 (6)	(i) 0.1581	0.1694	(i) 0.4099	0.4111 (2)	2.4	8.8
	(ii) −0.1720		(ii) 0.3407		(ii) 0.4068			

$M = (K_{0.5} + Yb_{0.5})$; an occupation of 0.5 corresponds to both (i) and (ii) positions.

Upon cooling, the highest-temperature phase α ($\mathbf{q} = 1\mathbf{b}^*$) transforms into the intermediate temperature phase β with $\mathbf{q} = (2/3 - \Delta)\mathbf{b}^*$, where $\Delta < 1/6$. The weak thermal effect detected on the DDSC curves is related to the switch of the $\mathbf{q}$ vector from 1 to 2/3. On further cooling $\mathbf{q}$ decreases continuously if the rate of cooling is slow enough to induce structure transformations. The lowest temperature phase γ ($\mathbf{q} = 1/2\mathbf{b}^*$) is a limiting member only in the corresponding sequence of structure transformations. This is why no thermal effect is observed in the γ–β phase transformation.

In this respect and within the frame of our method, phase β can be interpreted as a polytypic family of temperature-dependent members, each characterized by temperature-dependent $\mathbf{q}$ in the range between $1/2\mathbf{b}^*$ and $2/3\mathbf{b}^*$. The $\mathbf{q}$ vector is thus associated with the primary order parameter of the phase transition mechanism.

It is well known that

(i) the enthalpies of polytypic modifications are very close to each other and

(ii) the thermal treatments applied in their preparation guarantees that the samples are far from equilibrium.

Both (i) and (ii) lead to deviations from the general scheme of the phase transformations. Any incommensurate member of the $K_5Yb(MoO_4)_4$ family generated by the method described above contains mixed occupancy in the centre of M clusters (mixed M clusters). However, the commensurate members do not necessarily include them (Fig. 3, left column, and Fig. 7). It seems reasonable to propose that structures without mixed M clusters are stabilized by a relatively low cooling rate. Such a fully ordered commensurate structure should be considered as a lock-in phase, *i.e.* no other transformation of this phase could occur on further cooling. For example, the β–γ transformation could only occur at a slow cooling rate in order to allow for a
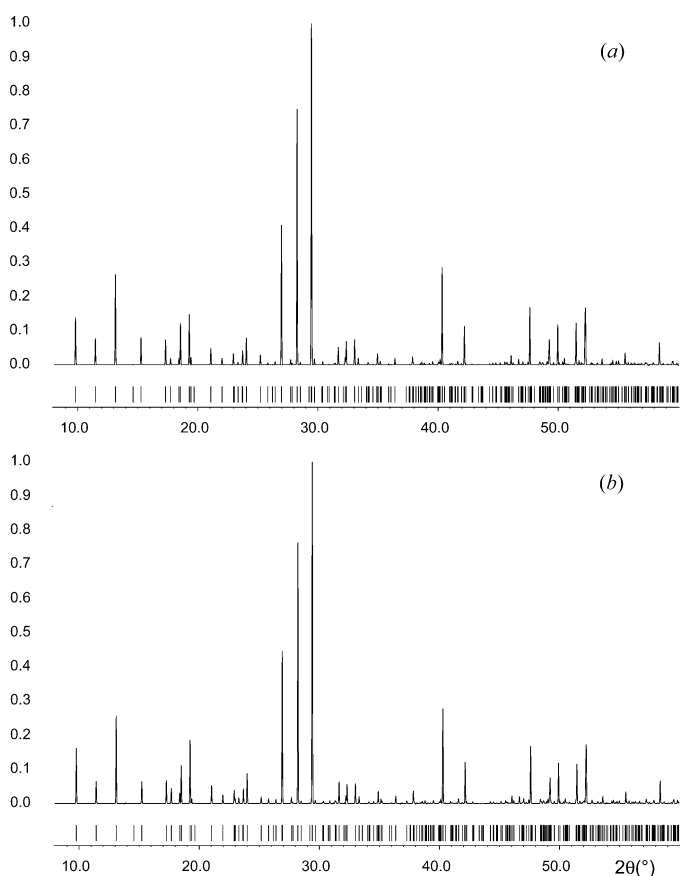

Figure 4
Powder diffraction diagrams calculated for (*a*) the simulated and (*b*) the experimental atomic parameters of phase γ. The unit-cell parameters obtained experimentally with Cu $K\alpha_1$ radiation (Morozov *et al.*, 2003) were used to generate the patterns.

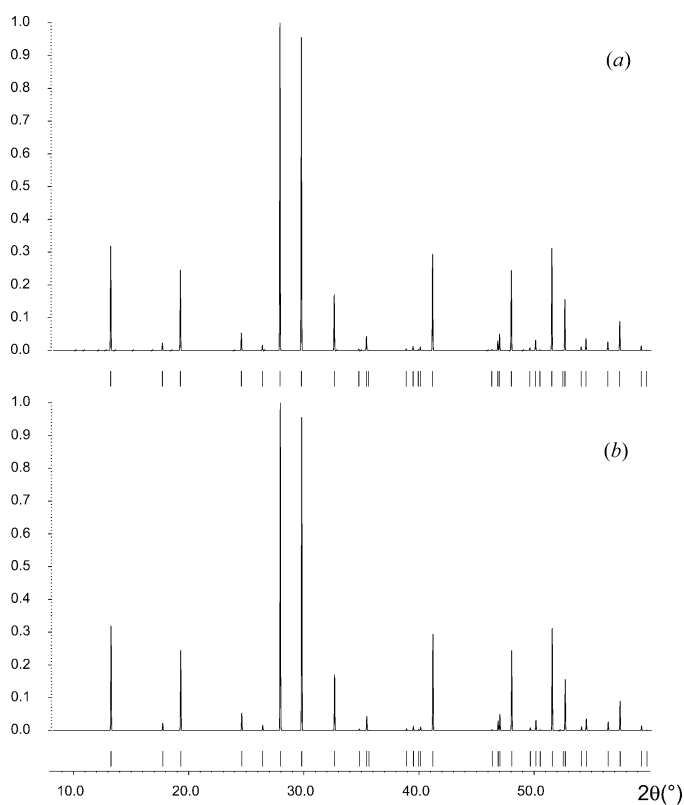**Figure 5**
Powder diffraction diagrams calculated for (*a*) the simulated and (*b*) the experimental atomic parameters of phase α. The unit-cell parameters obtained experimentally with Cu $K\alpha_1$ radiation (Morozov *et al.*, 2003) were used to generate the patterns.

progressive ordering of the M clusters. However, this process is terminated by the formation of the lock-in commensurate phase [$K_0Yb_{0.5}Yb_0K_{0.5}K_0Yb_{0.5}K_0K_{0.5}Yb_0Yb_{0.5}$] ($\mathbf{q} = 3/5\mathbf{b}^*$; Fig. 3$d$, left) before the commensurate phase γ [$K_0K_{0.5}Yb_0Yb_{0.5}$] ($\mathbf{q} = \frac{1}{2}\mathbf{b}^*$; Fig. 3$e$, left) can be reached. This explains why no $\beta \Rightarrow \gamma$ phase transition has been observed experimentally. On the other hand, heating the fully ordered γ phase always induces the formation of mixed M clusters, which explains why the $\gamma \Rightarrow \beta$ transformation was observed experimentally. Hence, the sequence of phase transformations depends
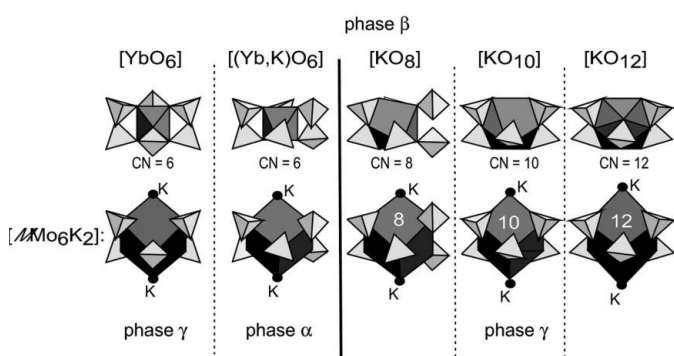

Figure 6
Correlation between the orientations of the MoO$_4$ tetrahedra in the M cluster and the coordination number (CN) of the MO_n polyhedron in phase β. Both M clusters and MO_n polyhedra are shown in dark grey. The MoO$_4$ tetrahedra are shown in light grey. As indicated, the clusters occur in the γ and the simulated α structures.
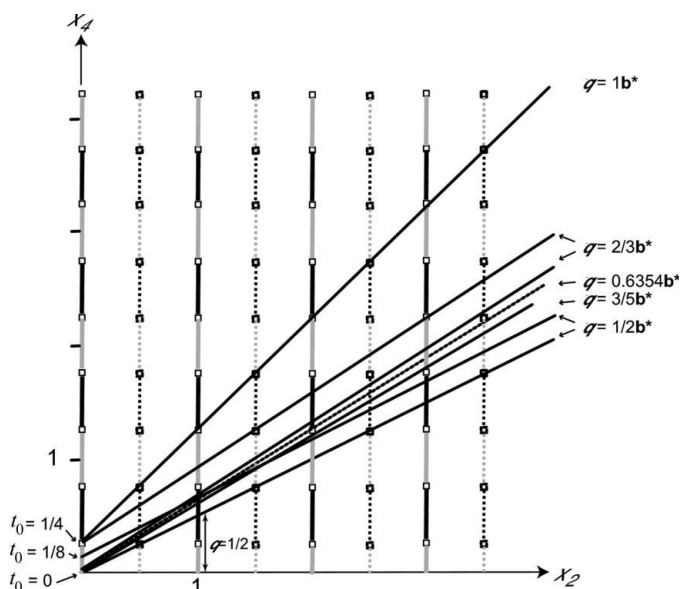

Figure 7
Occupation modulation of the M position in the x_2x_4 section of the incommensurate β phase along with a selection of the most probable simulated structures. Notations are analogous to Fig. 2. Each oblique line of the diagram corresponds to the b axis of a structure with its corresponding $\mathbf{q}$ vector given by the tangent of the slope angle. Solid lines show the b axes for some rational values (1/2, 3/5, 2/3 and 1$\mathbf{b}^*$) of $\mathbf{q}$; the irrational $\mathbf{q} = 0.6354\mathbf{b}^*$ refers to the refined structure of phase β (dotted line). For rational $\mathbf{q}$ vectors, the structure type depends on the value of t_0. This is illustrated for $\mathbf{q} = 2/3\mathbf{b}^*$ and $1/2\mathbf{b}^*$.

essentially on the thermal treatment, more specifically on the temperatures of annealing, and the cooling and heating rates. This confirms and explains the data obtained during the preparation of the difference phases described in §2.1.

In Fig. 3 some of the suggested phase-transformation paths are indicated with dashed arrows. For instance, the fully (100%) disordered α phase ($\mathbf{q} = 1\mathbf{b}^*$; Fig. 3$a$) could transform directly into a commensurate structure [$K_0Yb_{0.5}(K,Yb)_0K_{0.5}Yb_0(K,Yb)_{0.5}$] ($\mathbf{q} = 2/3\mathbf{b}^*$; Fig. 3$b$, right) if the cooling rate was fast enough to keep a third of the disordered mixed M clusters. Upon further cooling (decreasing the modulation vector $\mathbf{q}$), this structure should transform into an incommensurate one with a modulation vector in the range $2/3\mathbf{b}^* < \mathbf{q} < 3/5\mathbf{b}^*$. Two possible resulting structures, both commensurate ($\mathbf{q} = 3/5\mathbf{b}^*$; Fig. 3$b$) can be considered depending on the cooling rates. The first one is free of mixed M clusters [$K_0Yb_{0.5}Yb_0K_{0.5}K_0Yb_{0.5}K_0K_{0.5}Yb_0Yb_{0.5}$] (Fig. 3$b$, left), whereas the second one includes 20% of them [$K_0Yb_{0.5}Yb_0K_{0.5}(K,Yb)_0Yb_{0.5}K_0K_{0.5}Yb_0(K,Yb)_{0.5}$] (Fig. 3$b$, right). As mentioned above, the first structure does not allow any additional lower-temperature transformation. The second structure may further transform down to phase γ (Fig. 3e, left). Thus, the reversibility of the γ–β transformation depends on the thermal treatment.

With 50% of disordered M clusters and the minimal vector $\mathbf{q}$, the commensurate structure [$K_0(K,Yb)_{0.5}Yb_0(K,Yb)_{0.5}$] ($\mathbf{q} = 1/2\mathbf{b}^*$; Fig. 3$e$, right) can be considered as a possible high-temperature modification of phase γ.

5. Summary

A method to generate a family of modular structures from a single incommensurately modulated structure has been presented. This method takes advantage of the properties of the aperiodicity of the structure, which is completely characterized by the superspace formalism. It is based on the variation of the modulation vector $\mathbf{q}$ and, as an example, has been applied to the generation of the K$_5$Yb(MoO$_4$)$_4$ family. The validity of the proposed method was confirmed by comparison between the simulated and experimental structures. It is shown that the incommensurately modulated structure also contains information on the phase transitions of the compound. A consequent generalization of this approach explains the experimental data and predicts the behaviour of the compound under conditions at which it is far from thermodynamic equilibrium.

References

Arakcheeva, A., Chapuis, G., Petricek, V. & Morozov, V. (2005). *Acta Cryst.* B**61**, 400–406.

Elcoro, L., Perez-Mato, J. M., Darriet, J. & El Abed, A. (2003). *Acta Cryst.* B**59**, 217–233.

Lind, H. & Lidin, S. (2003). *Solid State Sci.* **5**, 47–57.

Morozov, V. A., Lazoryak, B. I., Lebedev, O. I., Amelinckx, S. & Van Tendeloo, G. (2003). *J. Solid State Chem.* **176**, 76–87.

Orlov, I., Schoeni, N. & Chapuis, G. (2004). *Superspace Group Finder*, Version 1.0. Laboratorie de Cristallographie, Lausanne, Switzerland. http://superspace.epfl.ch/finder/.

Petricek, V. & Dusek, M. (2000). *JANA*2000. Institute of Physics, Praha, Czech Republic.

Arakcheeva and Chapuis · Incommensurately modulated structures **59**